2 Search for Cold Dark Matter with CDMS-II

S. Arrenberg, L. Baudis, T. Bruch

in collaboration with: Department of Physics, Brown University, Department of Physics, California Institute of Technology, Department of Physics, Case Western Reserve University, Fermi National Accelerator Laboratory, Lawrence Berkeley National Laboratory, Massachusetts Institute of Technology, Department of Physics, Queen's University, Department of Physics, Santa Clara University, Department of Physics, Stanford University, Department of Physics, Syracuse University, Department of Physics, University of California, Berkeley, Department of Physics, University of California, Santa Barbara, Departments of Physics & Elec. Engr., University of Colorado Denver, Department of Physics, University of Florida, Gainesville, School of Physics & Astronomy, University of Minnesota, Minneapolis.

(CDMS-II Collaboration)

The Cryogenic Dark Matter Search (CDMS) experiment uses high-purity Ge (250 g) and Si (100 g) crystals kept at ∼20 mK to search for dark matter particles. Both phonons and electron-hole pairs are collected after a particle interacts in a crystal. Nuclear recoils produce less electron-ion pairs than electron recoils, thus the ionization yield, defined as $y \equiv E_{charge}/E_{recoil}$, is much smaller for nuclear recoils ($y \sim 0.3$ for Ge and ~ 0.25 for Si) than for electron recoils ($y = 1$) of the same energy. It provides the technique to reject the electron-recoil events which produce most of the background.

CDMS-II operates 5 towers (19 Ge and 11 Si detectors) with 4.5 kg of Ge and 1.1 kg of Si, in stable WIMP search mode since October 2006. Results from the data acquired between October 2006 and July 2007 (Runs 123-124), yielding an exposure of 121.3 kg d in Ge, have recently been published (1). A blind analysis resulted in zero observed events, the deduced upper limit on WIMP-nucleon spin-independent cross section is 4.6×10^{-44}cm^2 for a WIMP mass of 60 GeV/c^2 (1). It improves upon the sensitivity of XENON10 for WIMP masses above 42 GeV/c^2, providing the current best sensitivity above this mass.

Currently, the data from Runs 125-128, yielding an exposure above 400 kg d in Ge are under analysis. Our group was strongly involved in the analysis of the CDMS data Runs 123-124, and we are now focusing on the Runs 125-128. We have developed and are testing data reconstruction and quality cuts, as well as cuts regarding the event selection and topology. As examples, we mention the quality of the charge and phonon pulse reconstruction, the tests of detector behavior with time, the single-scatter cut, the charge threshold and the electron recoil band cuts. The preprocessing of Run 125-128 data is finished and these cuts are now applied and tested on calibration, as well as non-blind WIMP search data. The release of new results, with an expected sensitivity is $\sim 2\times10^{-44}$cm^2, is planned for summer 2009.

2.1 Search for solar axions with CDMS

Originally designed for WIMP searches, the CDMS-II experiment can also detect solar axions by Primakov conversion to photons. The Bragg condition for X-ray momentum transfer in a crystal allows for coherent amplification of the Primakov process. Since the orientation of the crystal lattice with respect to the Sun changes

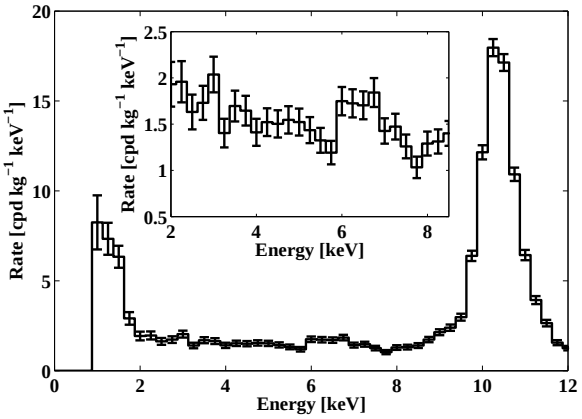

Figure 2.1: Co-added, efficiency corrected low energy spectrum of the Ge detectors considered in this analysis. The inset shows an enlargement of the spectrum in the analysis window, taken to be 2 to 8.5 keV.

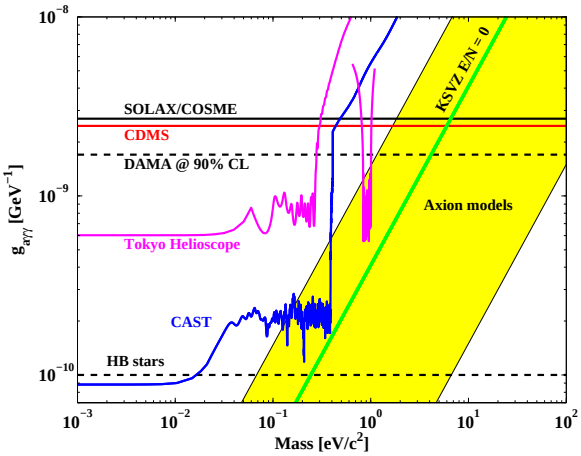

Figure 2.2: Comparison of the 95% C.L. upper limit on $g_{a\gamma\gamma}$ achieved in this analysis (red/solid) with other crystal search experiments (SOLAX/COSME [4; 5] (black/solid) and DAMA (upper black/dashed) [6]) and helioscopes (Tokyo helioscope (magenta/solid) [7] and CAST (blue/solid) [2]). The constraint from Horizontal Branch stars (lower black/dashed) is also shown [8].

with daytime an unique pattern of solar axion conversions is expected. The low background of ∼1.5 events/(kg d keV) (see Fig. 2.1)

and knowledge of the exact orientation of all three crystal axes with respect to the Sun make the CDMS-II experiment very sensitive to solar axions and, in contrast to helioscopes, the high mass region < 1 keV can be probed effectively. The result of an analysis of 289 kg-days of exposure resulted in a null observation of solar axion conversion. The analysis sets an upper limit on the axion photon coupling constant of $g_{a\gamma\gamma} < 2.6 \times 10^{-9}\,\mathrm{GeV}^{-1}$ at a 95% confidence level (Fig. 2.2). It inspires the prospects that future large crystal arrays such as SuperCDMS and GERDA may provide competitive sensitivity on the photon-axion coupling constant for $g_{a\gamma\gamma} < 10^{-9}\,\mathrm{GeV}^{-1}$ in the high mass region not easily accessible to helioscopes such as the CAST (2) experiment. A paper with the results has been submitted to PRL (3).

2.2 Effects of the Milky Way's dark matter disk on direct and indirect detection experiments

Recent simulation of hierarchical structure formation including the effect of baryons revealed that a thick dark matter disk forms in galaxies, along with the dark matter halo (9; 10). The dark disk has a density of $\rho_d/\rho_h = 0.25$ - 1.5 where $\rho_h = 0.3\,\mathrm{GeV/cm}^3$ and the kinematics are predicted to follow the Milky Way's stellar thick disk. At the solar neighborhood, this gives a rotation lag of $v_{lag} =$ 40 - 50 km/s with respect to the local circular velocity, and a dispersion of $\sigma \simeq$ 40 - 60 km/s. These velocities are significantly lower than in the standard halo model with v = 220 km/s and σ = 270 km/s. In collaboration with the group of Prof. G. Lake in the Theory Institute at UZH, we studied the impact of the low velocity of particles in the dark disk on direct and indirect dark matter detection.

For direct detection we find that the dark disk boosts the rates at low recoil energies, depending on the WIMP mass. As an example, for $M_W \gtrsim 50$ GeV, recoil energies of 5 - 20 keV and $\rho_d/\rho_h \leq 1$, the rate increases by factors up to 2.4 for Ge and 3 for Xe targets (Fig. 2.3).

Comparing this with the rates at higher energies will constrain the mass of the dark matter particle (M_W), particularly for $M_W > 100$ GeV. The dark disk also has a different annual modulation phase than the dark halo, while the relative amplitude of the two components varies with recoil energy and M_W. The increased expected dark matter flux improves the constraints on the WIMP cross section from current experiments. For likely dark disk properties ($\rho_d/\rho_h \leq 1$), the constraints for pure spin-independent coupling improve by up to a factor of 1.4 for CDMS-II, and 3.5 for XENON10. This work has been published in the Astrophysical Journal (11).

For neutrino telescopes, we find that the dark disk significantly boosts the capture rate of dark matter particles in the Sun and Earth as compared to the standard halo model (SHM). This increase owes to the higher phase space density at low velocities in the dark disk. For the Sun, the expected muon flux from the dark disk with $\rho_d/\rho_h = 1$ is increased by one order of magnitude relative to a pure SHM-generated flux. For the Earth — where WIMP capture and annihilation are not in equilibrium — the increase in the muon flux is two to three orders of magnitude, although this depends sensitively on the distribution function of the dark disk. Fig. 2.4 shows the summed muon flux at the Earth from the SHM and the dark disk as a function of the WIMP mass from neutrinos originated in the Sun, along with current experimental constraints and expected sensitivities for neutrino telescopes. The main results of these studies have been published in Physics Letters B (12). Our next goal is to quantify the impact of the dark disk on directional dark matter detectors.

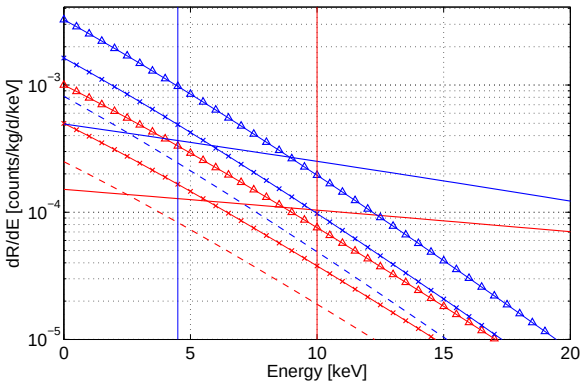

Figure 2.3: Differential recoil rates for Ge (red) and Xe (blue) targets, for WIMPs with $M_W = 100$ GeV and a cross section of 10^{-8} pb in the SHM (solid line) and the dark disk. Three different values of ρ_d/ρ_h (0.5 dashed, 1 $\times$ and 2 $\triangle$) are shown. Vertical lines mark current experiment thresholds: XENON10 (blue) using a Xe and CDMS-II (red) using a Ge target.

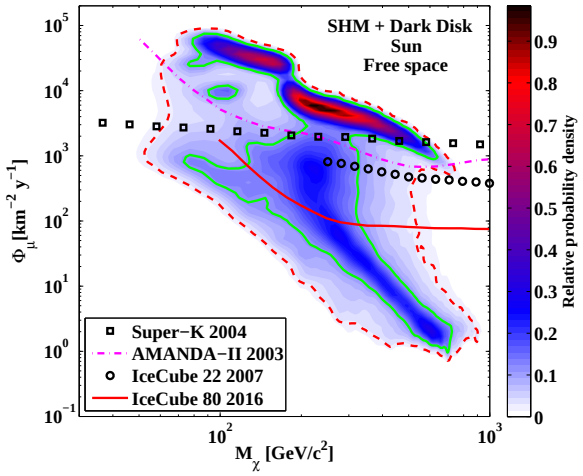

Figure 2.4: Summed muon flux at the Earth from the SHM and the dark disk as a function of the WIMP mass from neutrinos originated in the Sun. The closed contours show – 95% (red/dashed) and 68% (green/solid) – of the probability density of CMSSM models consistent with both astrophysical and collider constraints. The color-bar gives the relative probability density. Current experimental constraints on the muon flux from the Earth and Sun from Super-Kamiokande [13], AMANDA-II [14; 15] and IceCube22 [16] and the prediction for IceCube80 are also shown.

2.3 Analysis for inelastic dark matter and simulation of the WIMP velocity distribution

In direct search experiments dark matter particles in the galactic halo are usually described by a Maxwellian velocity distribution. This follows from the assumption that the dark halo is an isothermal sphere of collisionless particles. Another approach is to use the local velocity distribution of particles obtained from numerical simulations of Milky Way type halos. We are collaborating with the group of Prof. B. Moore in the Theory Institute to investigate the impact of velocity distributions obtained from the analysis of dark matter simulations on direct detection experiments. As shown in Fig. 2.5, the velocity distributions of dark matter particles tend to be broader and slightly suppressed at the peak, compared to the Maxwellian distribution. However, the impact on current limits from direct detection experiments is small, confirming that so far the Maxwellian approximation for the velocity distribution is a valid choice. This work is in progress, some of the goals being to study how many events we would need in an experiment in order to distinguish between different velocity distributions of WIMPs.

The observation of an annual modulation in the event rate by the DAMA collaboration was confirmed by the new DAMA/LIBRA results (17). The interpretation as a dark matter signal coming from standard WIMPs is in severe tension with results from all other direct detection experiments (18), as well as with indirect detection limits from Super-Kamiokande (19). One model which would allow to reconcile DAMA/LIBRA with other searches is the inelastic dark matter scenario (20). In this scenario, WIMP-nucleon scattering occurs only via inelastic scattering with the dark matter particle transiting into an excited state. Thus, only WIMPs with sufficient energy to up-scatter into the excited state can scatter off nuclei in the detector. The mass splitting between the WIMP and its excited state is considered to be a free parameter; in order to explain the DAMA/LIBRA results, the splitting needs to be around 120 keV (20). This model is still in agreement with all experiments, because it eliminates low energy events, the signal peaking at higher energies (for instance, at 70 keV in Ge and at 35 keV in I and Xe), a region which is often not analyzed for WIMP interactions. Our goal is to analyze the new CDMS data with respect to this model, including also the velocity distributions obtained from dark matter simulations discussed above. Figure 2.6 shows differential

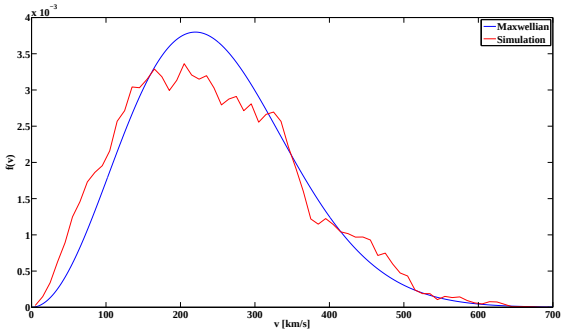

Figure 2.5:
Comparison of the velocity distribution from a particle sample from a simulation, 8 kpc away from the galactic center, with a Maxwellian distribution.

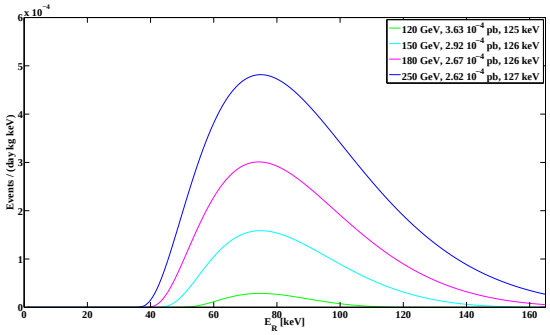

Figure 2.6: Differential event rates in the inelastic dark matter scenario. The numbers in the legend correspond to WIMP mass, WIMP-nucleon cross section and mass splitting, respectively.

rates for different WIMP masses, splittings and cross sections which are consistent with all experiments (20). In the standard WIMP scenario, the rates would be exponentially decreasing over the entire energy range.

[1] Z. Ahmed et al. (CDMS Collaboration), Phys. Rev. Lett. **102**, 011301 (2009).

[2] S. Andriamonje et al., J. Cosmol. Astropart. Phys. **04**, 010 (2007), E. Arik et al., arXiv:0810.4482.

[3] Z. Ahmed et al. (CDMS Collaboration), submitted to Phys. Rev. Lett., arXiv:0902.4693v1 (2009).

[4] F. T. Avigone et al., Phys. Rev. Lett. **81**, 5068 (1998).

[5] A. Morales et al., Astropart. Phys. **16**, 325 (2002).

[6] R. Bernabei et al., Phys. Lett. B **515**, 6 (2001).

[7] M. Minowa et al., Phys. Lett. B **668**, 93 (2008).

[8] G. G. Raffelt, Stars as Laboratories for Fundamental Physics, The University of Chicago Press (1996).

[9] J. I. Read, G. Lake, O. Agertz, V. P. Debattista, MNRAS **389**, 1041 (2008).

[10] J. I. Read, L. Mayer, A. M. Brooks, F. Governato, G. Lake, to be published in MNRAS, arXiv:0902.0009v1 (2009).

[11] T. Bruch, J. I. Read, L. Baudis, G. Lake, Astrophysical Journal **696**, 920-923 (2009).

[12] T. Bruch, A. H. G. Peter, J. I. Read, L. Baudis, G. Lake, Physics Letters B **674**, 250-256 (2009).

[13] S. Desai et al., Phys. Rev. D **20**, 083523 (2004).

[14] T. DeYoung et al. Journal of Physics: Conference Series **136**, 022046 (2008).

[15] A. Achterberg et al., Astropart. Phys. **26** 129 (2006).

[16] A. Karle et al. arXiv:0812.3981v1 (2008).

[17] R. Bernabei et al., Eur. Phys. J. C **56**, 333 (2008).

[18] Savage, Gelmini, Gondolo, Freese, arXiv:0808.3607v1 (2008), M. Fairbairn, T. Schwetz, arXiv:0808.0704v1 (2008), Aalseth et al., Phys. Rev. Lett **101** (2008), Behnke, Collar et al., Science **319** (2008).

[19] D. Hooper, F. Petriello, K. Zurek and M. Kamionkowski, arXiv:0808.246v4 (2008).

[20] S. Chang, G.D. Kribs, D. Tucker-Smith and N. Weiner, Phys. Rev. D **79**, 043513 (2009).